Frequency sensitivity in Hodgkin–Huxley systems

Yuguo Yu, Feng Liu, Wei Wang

National Laboratory of Solid State Microstructure and Department of Physics, Nanjing University, Nanjing 210093, People's Republic of China

Abstract. The frequency sensitivity of weak periodic signal detection has been studied via numerical simulations for both a single neuron and a neuronal network. The dependence of the critical amplitude of the signal upon its frequency and a resonance between the intrinsic oscillations of a neuron and the signal could account for the frequency sensitivity. In the presence of both a subthreshold periodic signal and noise, the signal-to-noise ratio (SNR) of the output of either a single neuron or a neuronal network present the typical characteristics of stochastic resonance. In particular, there exists a frequency-sensitive range of 30–100 Hz, and for signals with frequencies within this range the SNRs have large values. This implies that the system under consideration (a single neuron or a neuronal network) is more sensitive to the detection of periodic signals, and the frequency sensitivity may be of a functional significance to signal processing.

1 Introduction

Stochastic resonance (SR) is a phenomenon in which the responses of a nonlinear system to a weak periodic signal are optimized by suitable noise (Moss et al. 1993; Gammaitoni et al. 1998). In general, such nonlinear systems have a threshold, for example a system with a bistable potential, or an excitable sensory neuron. The SR can optimize the signal-to-noise ratio (SNR) of the output; the SNR first increases to a maximum and then decreases as the intensity of the external noise increases. In neural systems, the SR means that a neuron can utilize the environmental noise to process the input signals or stimuli (Wiesenfeld et al. 1994). A number of experiments on various neural systems have been reported showing such a nonlinear phenomenon (Douglass et al. 1993; Bulsara et al. 1993; Bezrukov et al.

1995; Wiesenfeld and Moss 1995; Collins et al. 1996a,b; Cordo et al. 1996; Levin and Miller 1996; Gluckman et al. 1996). These include studies of single mechanoreceptive sensory neurons from crayfish (Douglass et al. 1993; Wiesenfeld and Moss 1995) and rat skin (Collins et al. 1996b), single interneurons from cricket abdominal ganglia (Levin and Miller 1996), and a network of neurons from the mammalian brain (Gluckman et al. 1996). The occurrence of the SR has been argued as the ability to detect and to transduce or encode weak signals.

Recently, the phenomenon of frequency sensitivity in weak-signal detection has been examined both experimentally (Levin and Miller 1996) and theoretically (Wang et al. 1998; Liu et al. 1999). It was found that there exists a frequency-sensitive range below 100 Hz. In this range the coherence of the spike response of the neurons to an input signal is evidently enhanced, improving the neurons ability for detection and transduction of the signal (Levin and Miller 1996). In addition, it was also suggested that the SR could enhance the effects of weak intrinsic rhythmic oscillations such as the θ rhythm (4–10 Hz) or, more widespread, the γ rhythm (30–100 Hz) in the brain (Gluckman et al. 1996).

To further explore how such frequency sensitivity relates to the intrinsic nonlinear features of the neuronal system, we present a study based on a popular neuronal model: the Hodgkin–Huxley (HH) model (which represents the typical firing dynamics of a real neuron). By numerical simulations we show that there is a frequency-sensitive range range of 30–100 Hz in both a single HH neuron and a network (which consists of a number of HH neurone), and in this range the SNRs have large values. We argue that this results from the resonance between the intrinsic oscillation of the system and the input signal. The dependence of the critical amplitude of the periodic input signal upon its frequency and the coherence resonance in a single neuron show the existence of an intrinsic oscillation (Wang et al. 1998; Lee and Seunghwan 1999; Liu et al. 1999), which is due to the nonlinear dynamic features of the neuronal model. The phenomenon of the frequency sensitivity to input

Correspondence to: Y. Yu

signals may be important for signal processing in the neural system Whittington et al. 1995), and should have some obvious effects on the responses of the neurons to the external stimuli.

This paper is organized as follows. In Sect. 2 the single HH neuronal model and the network consisting of the HH neurons are described. The results and discussions for the frequency sensitivity of the single neuron are presented in Sect. 3, while those for the network are given in Sect. 4. Finally, a conclusion is given in Sect. 5.

2 Model

The HH neuronal model was originally introduced to describe the dynamic behavior of the squid's giant axon (Hodgkin and Huxley 1952). Later, the HH neuron was regarded as a useful paradigm to account naturally for both the spiking behavior and refractory properties of real neurons, and it serves as a starting point for modeling more complex dynamical behaviors such as bursting of spikes. A HH neuron is described by four coupled nonlinear equations: one for the membrane potential V and the other three for the gating variables: m, n and h; that is,

$$\frac{dV}{dt} = (I_{ext}(t) + I_{ion}(t))/C_m \ , \tag{1}$$

$$\frac{dm}{dt} = (m_\infty(V) - m)/\tau_m(V) \ , \tag{2}$$

$$\frac{dh}{dt} = (h_\infty(V) - h)/\tau_h(V) \ , \tag{3}$$

$$\frac{dn}{dt} = (n_\infty(V) - n)/\tau_n(V) \ , \tag{4}$$

with

$$I_{ion}(t) = -g_{na}m^3h(V - V_{na}) - g_k n^4(V - V_k) \\ - g_1(V - V_1) \ , \tag{5}$$

$$I_{ext}(t) = I_0 + I_1 \sin(2\pi f_s t) + \xi(t) \ . \tag{6}$$

The ionic current I_{ion} includes the usual sodium (I_{na}), potassium (I_k), and leak (I_1) currents. The parameters g_{na}, g_k and g_1 are the maximal conductances for the ion and leakage channels, and V_{na}, V_k, V_1 are the corresponding reversal potentials. In addition, m_∞, h_∞, n_∞, and τ_m, τ_h, τ_n represent the saturation values and the relaxation times of the gating variables, respectively. Detailed parameter values can be found in Hodgkin and Huxley (1952) and Hansel et al. (1993).

The neurons always receive synaptic inputs from other neurons, and also have various fluctuations in their own membranes. If the total inputs from the environment vary slowly with time, these inputs can be assumed to be a constant current I_0 (subthreshold or suprathreshold) (Wang et al. 1998; Liu et al. 1998). The term $I_1 \sin(2\pi f_s t)$ is a subthreshold input signal, i.e., it alone is insufficient to evoke firing of the neuron. In view

of the complex origins of noise, $\xi(t)$ is chosen as Gaussian white noise, with

$$\langle \xi(t) \rangle = 0, \quad \langle \xi(t_1)\xi(t_2) \rangle = 2D\delta(t_1 - t_2) \ , \tag{7}$$

where $\langle \ldots \rangle$ represents the ensemble average and D represents the noise intensity. Thus, I_{ext} is the total external stimulus injected into the neuron.

For a network with a number of neurons, the synaptic interaction between the neurons can be modeled as follows. The spike or burst firing of a neuron always affects other connected neurons. To include this synaptic effect, one must add a synaptic current I_{syn} to the right-hand side of (1) for the evolution of the membrane potential. In the following we use the simplest way to model these multiple events (Segev et al. 1989).

The dynamic equations for the network consisting of a number of the HH neurons could be presented as follows:

$$\frac{dV^i}{dt} = (I_{ext}^i(t) + I_{ion}^i(t) + i_{syn}^i(t))/C_m \\ i = 1, 2, \ldots N \tag{8}$$

where the ionic current I_{ion}^i and the external stimulus current I_{ext}^i are the same as defined for the case of single neuron. The synaptic current I_{syn}^i is described by:

$$I_{syn}^i(t) = -\frac{1}{N} \sum_{j=1, j\neq i}^{N} g_{syn}\alpha^i(t - t^j)(V^i - V_{syn}^{ij}) \ , \tag{9}$$

with

$$\alpha^i(t) = (t/\tau)\exp[-t/\tau] \ . \tag{10}$$

In Eq. (9), g_{syn} is the peak synaptic conductance and V_{syn}^{ij} is the synaptic potential between the i-th neuron and the j-th one, τ is the characteristics time of the synaptic interaction, and t^j is the instant when the interaction starts, i.e., the time of the firing of a spike by the presynaptic neuron j. Here, all times delays are neglected.

The synaptic effect is traditionally classified as excitatory or inhibitory depending on the value of V_{syn} with respect to the resting potential V_{eq} (which is about -65 mV when $I_0 = 0$, i.e., the potential of neuron at the quiescent state). If the interaction is excitatory, i.e., $V_{syn} > V_{eq}$, we have $I_{syn} > 0$ over most of the potential range ($V_k < V < V_{na}$). This tends a priori to induce firing in the postsynaptic neuron. Differently, in the inhibitory case ($V_{syn} < V_{eq}$), the interaction tends to hyperpolarize the target neuron and to stabilize it in a quiescent state (Hansel et al. 1993). In this work, for the interaction (or the coupling) between any two neurons, we let V_{syn} be randomly equal to either -80 mV or 0 mV, with -80 mV for an inhibitory coupling and 0 mV for an excitatory one. The ratio of the inhibitory couplings to the excitatory ones, i.e., the percentage of the inhibitory couplings in the total number of the synaptic couplings, is assumed to be 0.33 (Wang et al. 1997a), which is suitable for synchronized oscillations of the neurons in

the network. The number of neurons in the network is taken to be $N = 100$.

The output of the network is defined as

$$V^{\text{out}}(t) = \frac{1}{N} \sum_{i=1}^{N} \theta(V^i(t) - V^*) \ . \tag{11}$$

Here we consider the average of the firing activities of all neurons as the output of the network, which may encode the input signal. In (11), V^* is a membrane potential threshold, and $\theta(x) = 1$ if $x \geq 0$ and $\theta(x) = 0$ if $x < 0$. The numerical integration of the equations described above is performed using the second-order algorithm suggested by Fox (1991), and the integration step is taken to be 0.03 ms. The final results concerning the calculation of the power spectal densities (PSDs) and the SNRs are obtained by taking an average over 100 different simulations. Here, such an ensemble averaging is to model the long time presentation of the signals and to eliminate the statistical fluctuations on the output of the neurons. On the other hand, such an averaging is also considered the effect of the huge number of neurons for the network case. We note that such calculations of the PSD and the SNR are similar to those used in the literature (for example: Gluckman et al. 1996; Levin and Muller 1996).

3 Single neuron case

Let us discuss the dynamics of a single neuron first. When a small step current $I_0(I_0 < 6.2 \, \mu\text{A/cm}^2)$ is applied, the membrane potential undergoes a subthreshold damping oscillation with a frequency between 50 and 85 Hz (see Fig. 1a,b) to a stable fixed point with $V_{\text{eq}} = -65 \, \text{mV}$. It is found that the frequency of such an oscillation increases monotonically as the value of I_0 increases. Obviously, this subthreshold oscillation manifests an intrinsic feature of the neuron, i.e., an intrinsic oscillation. The birth of limit cycles, resulting from a Hopf bifurcation, occurs at $I_0 = I_c \approx 6.2 \, \mu\text{A/cm}^2$, and leads to the firing of spikes (when $I_0 \geq I_c$) (Lee et al. 1998). Figure 1c shows an example of the limit cycle. The minimal frequency of firing is about 50 Hz at $I_0 = I_c$, which is discontinuous to that of the subthreshold oscillation due to the Hopf bifurcation. Starting from its minimal value of about 50 Hz, the frequency of firing increases monotonically as I_0 increases. The periodic firing of spikes stops at $I_0 = 154.5 \, \mu\text{A/cm}^2$, where the fixed point becomes stable again through a normal Hopf bifurcation (Hansel et al. 1993).

Recently it has been shown that the nonlinear system with noise can exhibit the SR-like behaviors even without external signals. This phenomenon is called *coherence resonance* (CR) (Pikovsky and Kurths 1997). Clearly, for $I_0 < I_c$, subthreshold oscillations can excite firing of spikes when noise of a suitable intensity is applied. We expect that these firings will have frequencies located in the same range of the frequencies shown in Fig. 1a. Figure 2a shows the PSD of the firings for different subthreshold stimuli I_0 in the case of the noise
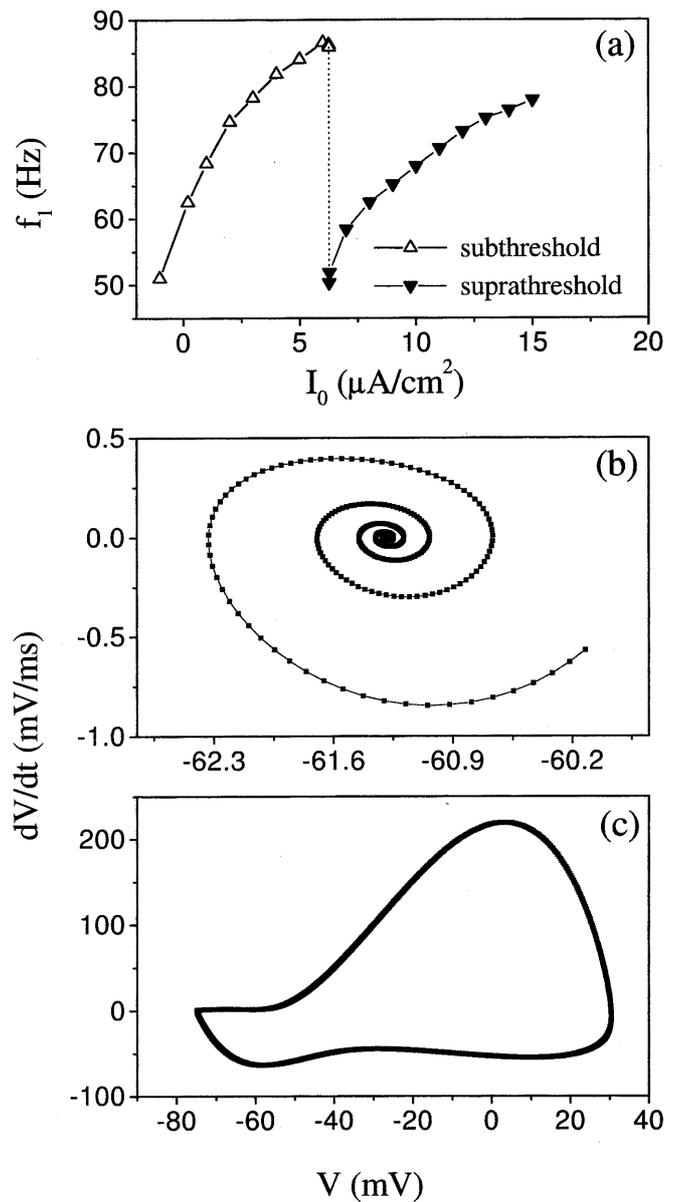

Fig. 1. **a** The frequency of periodic output of a neuron versus the step current I_0. For $I_0 < 6.2$, f_1 is the frequency of the subthreshold oscillation, and for $I_0 > 6.2$, f_1 is the frequency of the periodic firing. **b** Phase plot of dV/dt versus V with $I_0 = 5$ in which the trajectory moves clockwise around the loop, and the equilibrium state is a global attractor. **c** Phase plot of dV/dt versus V in the case of $I_0 = 10$ in which the trajectory moves clockwise around the loop and is a limit cycle

intensity $D = 2$. (Here the firings of spikes in the neuron have been converted into a time series of standard pulses $V(t)$ with $V_1 = 1.0$, with a width of $\Delta\tau = 2$ ms and $V_0 = 0$ related to the firing and nonfiring states, respectively. The time series is then transformed into a power spectrum through the fast Fourier transformation.) Figure 2a shows several peaks for each stimulus I_0. These peaks reflect the CR between the intrinsic oscillations and the noise, and especially the main peak (or the peak with low frequency) characterizes the CR. The frequency of the main peak is limited to a range of 30–100 Hz. When the value of I_0 increases, the main peak
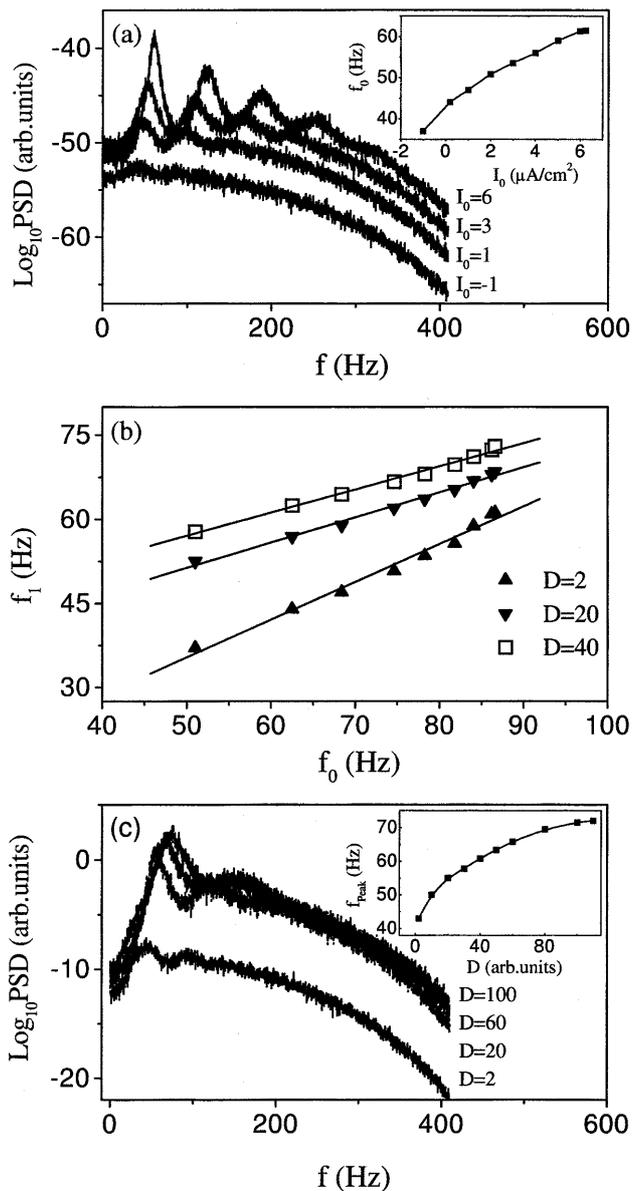
Fig. 2. a Power spectral density (PSD) at the output of a neuron for $I_0 = -1$, 1, 3, and 6. *Inset*: the frequency f_0 of the peak of each power spectrum versus the step current I_0, in the presence of noise with intensity $D = 2$. **b** Correlation between the peak frequency f_0 of the Coherence resonance with three noise intensities ($D = 2$, 20, and 40) and the frequency f_1 of the subthreshold oscillation. **c** PSD at the output of the neuron in the presence of noise with intensities $D = 2$, 20, 60 and 100. *Inset*: The frequency f_{peak} of the peak in each power spectrum versus the noise intensity D with $I_0 = 0$

the existence of the intrinsic oscillations is a general feature of excitable neuronal systems. As a matter of fact, the oscillations could be induced by various inputs, e.g., a noise or an effective stimulus. It is this intrinsic feature that enables the neuron to display a special frequency sensitivity ranging from 30 to 100 Hz. A different noisy environment only enables the neuron to fire with a slightly different frequency. When a periodic signal is applied to a neuron, the modulation between the intrinsic oscillation and the signal will make it easy for the neuron to fire within an appropriate frequency range related to the signal frequency.

Figure 1a shows how the frequencies of the sub-threshold oscillations vary with input I_0, while Fig. 2a shows how the frequencies of the main peaks of the noise-induced coherent oscillations vary with I_0. For the cases shown in Fig. 2a, we add an additional weak noise to the neuron. It is interesting to examine the relation between the subthreshold oscillation and the noise-induced firings of the CR. Figure 2b gives the correlation between the frequencies f_0 of the main peaks of the CR (in the case of three values of noise intensity D) and the frequencies f_1 of the subthreshold oscillations for a single neuron. With equal noise intensity D, for different subthreshold input I_0, there is an excellent linear relationship (with correlation coefficient $r > 0.99$) between f_0 and f_1. Note that for obtaining f_0, we need to add both a subthreshold input I_0 and a noise with intensity D to the neuron, while for f_1 we only add the subthreshold input I_0 to the neuron. Thus, we plot these two frequencies together in Fig. 2(b). The perfect linear relation reflects that both kinds of oscillations, i.e., the sub-threshold oscillation and the CR, have the same physical origin, namely the intrinsic oscillation (Wang et al. 1998). Indeed, the subthreshold oscillation is a sub-threshold manifestation of the intrinsic oscillation, which can bee affected by I_0. Differently, the CR is a suprathreshold manifestation of the intrinsic oscillation, i.e., the intrinsic oscillation induced as the firing of spikes by the current I_0 and noise. Thus, the CR related to the firing of spikes preserves the frequency characteristic of the intrinsic subthreshold oscillation if the existence of the noise only affects the near-threshold dynamical behavior of the neuron, i.e., the noise level is still low. It is also worth noting that since each point in Fig. 2b is plotted for one value of I_0, at a certain level of noise D, all points should fall on a line because of the near-threshold dynamical behavior. In addition, from Fig. 1a and Fig. 2a one can see that both curves of f_1 versus I_0 and f_0 versus I_0 have basically the same monotonic behavior. Clearly, the linear relation will be destroyed by a large current I_0 and a high level of noise.

Actually, the mechanism of CR in neuronal models has been discussed in detail by Pikovsky and Kurths (1997) (for the FitzHugh-Nagumo model) and by Lee et al. (1998) (for the HH neuron). It is argued that the existence of a subthreshold oscillation (e.g., a focus-type state of equilibrium) is a necessary condition for a peak to occur in the spectral density at a non-zero frequency. Besides the observation of dependence of the peaks in the PSD on the noise intensity (Hu et al. 1993; Pikovsky

shifts to a range with high frequency. The inset of Fig. 2a shows the frequencies f_0 of the main peaks in the range of 30–70 Hz for various values of I_0 in the case of $D = 2$. When the noise intensity D increases, this frequency range shifts to 50–90 Hz (not shown here). Since the noise is white, the peaks of the PSD are an inevitable reflection of the intrinsic behavior of the excitable neurons or of the excitation of the intrinsic oscillations. This behavior was also found in the Hindmarsh-Rose neuronal model and the Bahoeffer-van der Pol model (Wang and Yao 1992; Wang et al. 1997a). All these imply that

and Kurths 1997; Lee et al. 1998) (see also Fig. 2c), we would like to point out that with a fixed noise intensity, the frequencies of the peaks in the PSD also vary with the current I_0. The mechanism described by Lee et al. matches for the parameter I_0 near the onset of the saddle-node bifurcation of periodic orbits (i.e., near the firing threshold of the neuron). As discussed in a number of papers (Hänggi et al. 1990; Gammaitoni et al. 1998; Lee et al. 1998), the dynamic properties of a noise-driven HH neuron are similar to the Kramers transition of a damped particle between two wells of the double-well potential. The additional weak noise is treated as the fluctuational force that causes transitions of the particle between the potential wells. The dynamic firing of the HH neuron corresponds to the crossing of a particle over a potential barrier. In the HH neuronal system, there are two time scales in the presence of the sub-threshold current I_0 and the weak noise within density D. One is the period of the subthreshold oscillation, which is determined by I_0. The other is the mean time to drive the system from its stable point to the limit-cycle region, or the activation time, which is similar to the Kramers time (Hänggi et al. 1990; Gammaitoni et al. 1998). for a fixed value of I_0, when the noise intensity increases to an optimal level, the noise-induced activation time approaches a value that is matchable to the period of the intrinsic oscillation of the neuron. This results in the maximal coherent motion of the neuron, i.e., the manifestation of the CR. The detailed descriptions of the mechanism underlying CR in neuronal models are given in Hänggi et al. (1990), Gammaitoni et al. (1998), and Lee et al. (1998).

Now we study the responses of a neuron to the periodic signals. With a subthreshold current I_0, when the HH neuron is subjected to an additional periodic signal $I_1 \sin(2\pi f_s t)$, there is a threshold amplitude for the firing of spikes $I_{1c} = I_{1c}(f_s)$. This threshold amplitude separates the phase diagram of amplitude and frequency of the signal into nonfiring and firing regions, as shown in Fig. 3. When $I_1 < I_{1c}(f_s)$ there is no firing of spikes, while for $I_1 \geq I_{1c}(f_s)$ the system shows complex dynamic behavior including periodic firings with mode-locking states and irregular spiking patterns. Since I_0 could be considered to be the effect of the environment in which the neuron is located, we have $I_0 = -1$ for an inhibitory environment and $I_0 = 1$ for an excitatory one. Obviously, only the presence of I_0 cannot evoke neuron to fire. But it can drive the neuron from its quiescent state to a sensitive state for the signal transduction. We note that for the three curves shown in Fig. 3 there is a common most sensitive range of 30–100 Hz (see also in Fig. 4). In this range the neuron will fire with a smaller value of I_1. As a matter of fact, this frequency range results from a resonance between the intrinsic oscillation and the periodic signal (Wang et al. 1997b). The input periodic signal will transfer more energy to the neuron to evoke the firing of spikes when both frequencies are matched. In the following we show that within this sensitive range, the detection and transduction abilities of the neurons to weak periodic input signals are significantly improved in the presence of a weak noise.
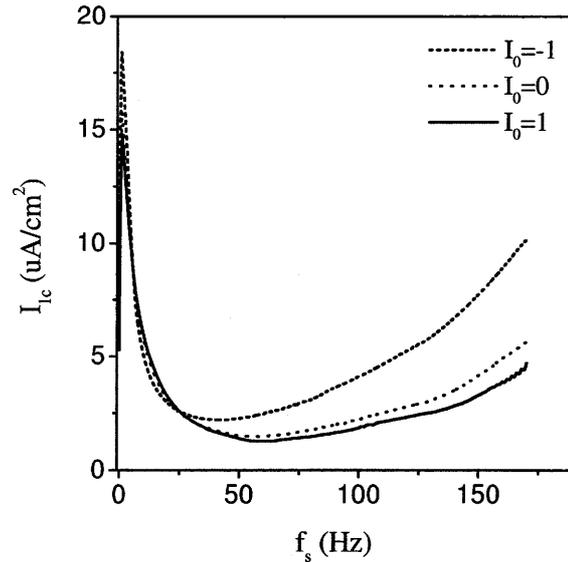

Fig. 3. The threshold amplitude I_{1c} versus signal frequency f_s for $I_0 = 0$, -1, and 1

In order to study the responses of the neurons located in a noisy environment to periodic signals at different frequencies, we assume that the signal amplitude I_1 and the current I_0 are identical for each frequency. At the same time, all the signals are kept as subthreshold (here I_1 is taken as 0.9 and $I_0 = 1$). That is, when subjected to a subthreshold periodic signal, the neuron can be evoked to fire only by noise. The SNR of the firings is calculated to quantify this noise-induced firing effect. Figure 4a shows the dependence of SNRs at the output of the neuron on the noise intensity D, in the case of three input signals with $f_s = 10$, 40, and 120 Hz. The relationships present clearly the typical characteristic of the SR: first a rise and then a drop. The maximal SNR is obtained around $D \approx 2$ in the case of $f_s = 40$ Hz. This can be understood as follows. When a small noise is added to a neuron, the SNR rises rapidly from zero. This is because noise easily induces firing of the neuron. The firing shows a strong coherence with the signal, i.e., the neuron always fire spikes when the periodic signal is around its maxima. Therefore, the SNR rises and reaches its maximum at an optimal noise intensity. Differently, in the case of large noise, firing shows a rather random behavior, and the output carrying the component of the input signal is almost buried in the noise. Thus, the SNR drops quickly or even disappears. Obviously, the SNR for $f_s = 40$ Hz is always larger than that for $f_s = 10$ Hz and $f_s = 120$ Hz. On the other hand, the differences in SNR between various frequencies at a small noise intensity are much larger than those at a large noise intensity, since in the latter case the noise dominates the firing dynamics of the neuron. This is shown in Fig. 4b.

Figure 4b shows the SNR versus the frequency of the input signal for $D = 1$ and $D = 10$. The SNRs for the frequencies located around 60 Hz have large values. This implies that the neuron is more sensitive to the signals with frequencies in the range of 30–100 Hz. Physically, this is due to the resonance between the intrinsic
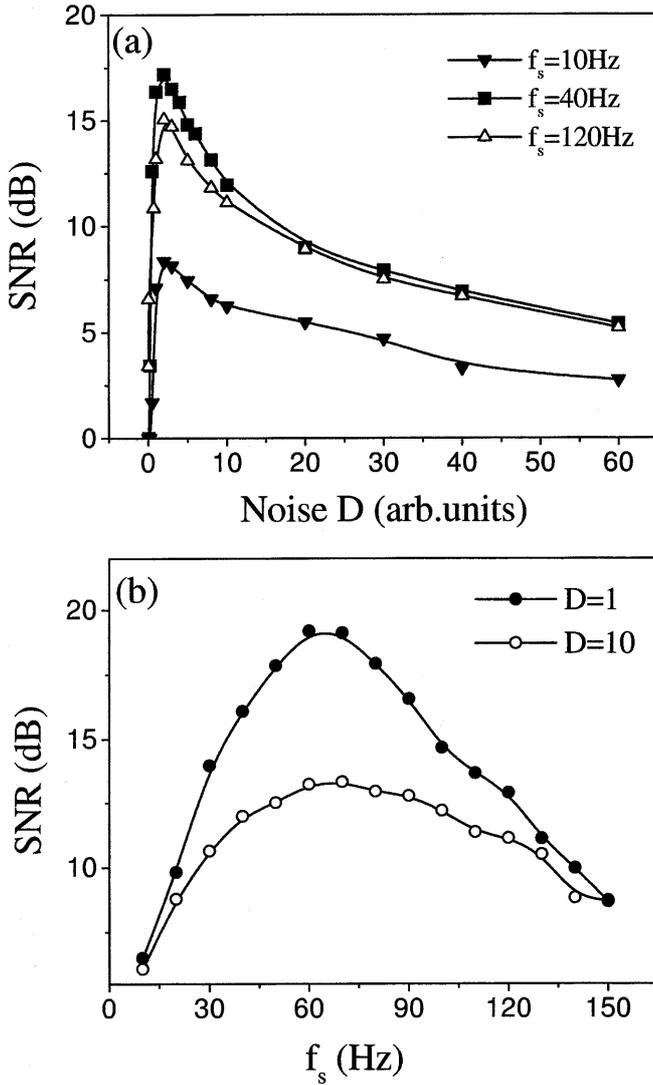
232

Fig. 4. a The Signal-to-noise-ratio (SNR) of the single neuron versus the noise intensity D for periodic signals with frequencies $f_s = 10$, 40, and 120 Hz (with $I_0 = 1$ and $I_1 = 0.9$). **b** The SNR of the single neuron versus the signal frequency f_s for two noise intensities $D = 1$ and $D = 10$ (with $I_0 = 1$ and $I_1 = 0.9$)

oscillation and the periodic signal (see Fig. 3), by which the neuron fires spikes around the maxima of the signal and more noise energy is transferred to the neuron to evoke the firing of spikes. As a result, the SNR at the output of the neuron for a signal with a frequency in the range of 30–100 Hz is high, which suggests that the ability to detect and transduce the signal can be significantly improved in the presence of a weak noise as long as the frequency falls within such a range.

4 Neuronal network case

We now turn to the frequency sensitivity in a globally coupled network with excitatory and inhibitory couplings. Here we consider a simple case in which all neurons are assumed to have identical values of I_0 and signal strength I_1, e.g., $I_0 = 1$ and $I_1 = 0.9$. The effective stimulus strength for each neuron is
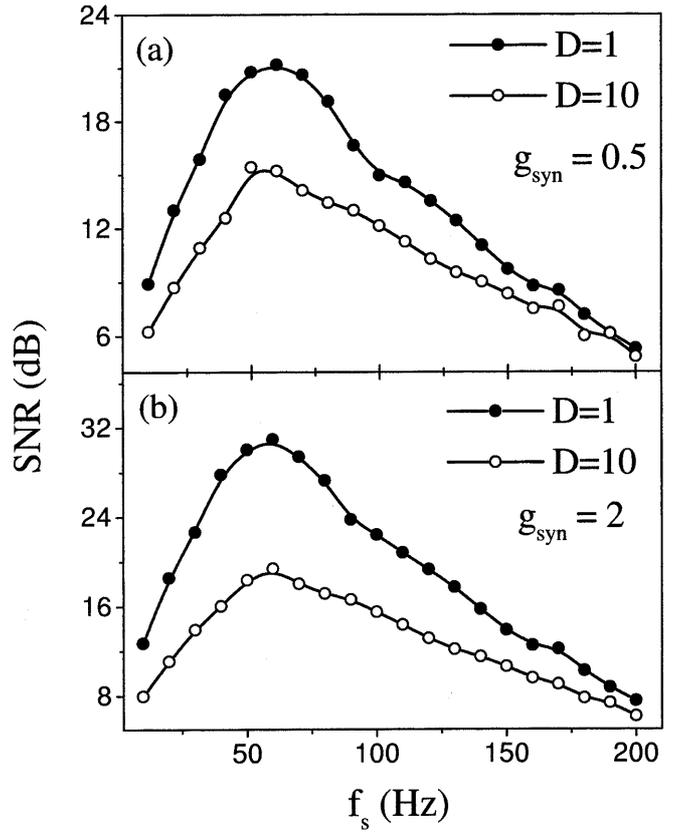

Fig. 5a,b. The SNR of the first neuron in the network versus the signal frequency f_s for two coupling strengths, $g_{syn} = 0.5\,\mathrm{mS/cm^2}$ (**a**) and $g_{syn} = 2\,\mathrm{mS/cm^2}$ (**b**), for $D = 1$ and $D = 10$ (with $I_0 = 1$ and $I_1 = 0.9$)

$$I_{eff}^i(t) = -\frac{1}{N}\sum_{j=1,j\neq i}^{N} g_{syn}\alpha^i(t - t^j)$$
$$\times (V^i - V_{syn}^{ij}) + I_0 + I_1 \sin(2\pi f_s t) \ . \tag{12}$$

When a number of neurons are coupled into a network, every individual neuron within the network will have the same features as discussed in Sect. 3, but with different effective stimuli (see Eq. 12). For a neuron in the network, there is also a sensitive range as shown in Fig. 5. The SNRs are larger than those in Fig. 4b. Furthermore, the SNRs for strong couplings, e.g., $g_{syn} = 2\,\mathrm{mS/cm^2}$, are larger than those of weak couplings, e.g., $g_{syn} = 0.5\,\mathrm{mS/cm^2}$, (see Fig. 5a and b, respectively). The effect of the signal transduction is shown by means of the average synaptic input (Lindner et al. 1996):

$$I_{syn}(t) = -\frac{1}{N^2}\sum_{i=1}^{N}\sum_{j=1,j\neq i}^{N} g_{syn}\alpha^i(t - t^j)$$
$$\times (V^i - V_{syn}^{ij}) \ . \tag{13}$$

As shown in Fig. 6 $I_{syn}(t)$ presents a periodic feature (for a small noise with $D = 2$). It is this periodic synaptic current that enhances the firings and then results in an increase in the SNR (Liu and Seunghwan 1999). Here, the coupling strength plays an important role.

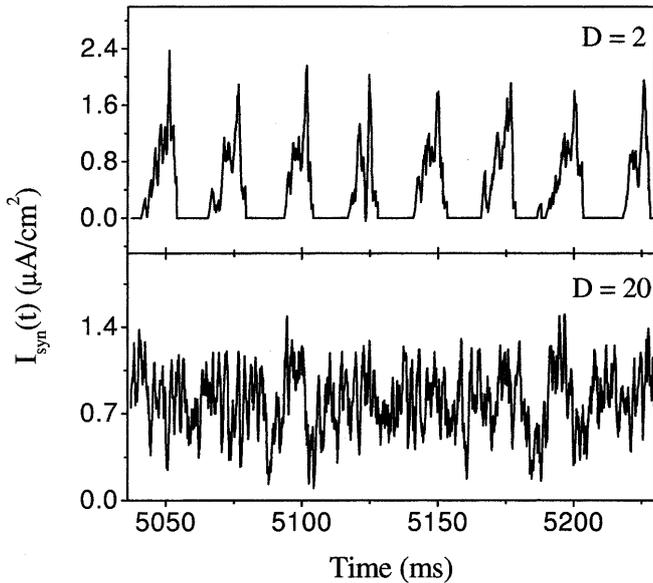The intensity and quality of $I_{syn}(t)$ also depend on the intensity of the noise, as shown in Fig. 6. Now we input

Fig. 6. Average synaptic input $I_{\text{syn}}(t)$ versus time for two noise intensities $D = 2$ (*upper*) and $D = 20$ (*lower*). The coupling strengths in both cases are $g_{\text{syn}} = 2\,\text{mS/cm}^2$ and the signal frequency is $f_{\text{s}} = 40\,\text{Hz}$ (with $I_0 = 1$ and $I_1 = 0.9$)

Fig. 7. a The SNR of the network versus noise intensity D for three signals with $f_{\text{s}} = 10$, 40, and 120 Hz. **b** The SNR of the network versus signal frequency for two noise intensities $D = 1$ and $D = 10$. For both figures $g_{\text{syn}} = 0.5\,\text{mS/cm}^2$, $I_0 = 1$, and $I_1 = 0.9$

a signal with frequency $f_{\text{s}} = 40$ Hz to the network with fixed coupling strength $g_{\text{syn}} = 2$. When the noise intensity is very weak, e.g., $D < 0.5$, peaks in $I_{\text{syn}}(t)$ are only present around the maxima of the signal. The peaks are often separated by several periods, and apparently the heights of these peaks also vary. When the noise intensity increases to an optimal intensity, near $D = 2$, $I_{\text{syn}}(t)$ present a pulse-like shape and varies with the same period as that of the signal. The heights of the peaks in $I_{\text{syn}}(t)$ are of the order $1.5 \sim 2.5$, which are larger than the amplitude of the signal (See Fig. 8a). Accordingly, the neurons fire spikes when the signal is around its maximum, i.e., their firing is more tightly phase-locked to the signal. Thus, the SNR at the output of a neuron in the network is larger than for a neuron at a lower noise intensity. As the noise intensity further increases, e.g., $D \geq 20$, $I_{\text{syn}}(t)$ contains an evidently random component, as shown in Fig. 6. The peaks in $I_{\text{syn}}(t)$ are broader in width and lower in height. This implies that the neurons fire spikes somewhat randomly. Thus the SNR at the output of a neuron in the network decreases, and so does the quality of $I_{\text{syn}}(t)$. In short, the couplings between the neurons, together with a suitable weak noise, have the effect of an enhancement in the ability to detect and transduce weak periodic signals.

Figure 7a shows the SNRs of the network for signals with frequencies $f_{\text{s}} = 10$, 40, and 120 Hz. In all the cases the SNR first rises sharply and then drops as the noise intensity increases, which is the typical characteristic of SR. As a matter of fact, the dependence of the output of the network $V^{\text{out}}(t)$ on the noise intensity resembles that of $I_{\text{syn}}(t)$. At a low noise level, $V^{\text{out}}(t)$ presents sharp peaks when the signal is around its maxima, and these peaks are of large amplitude. In the case of noise, V^{out} contains a random component (determined by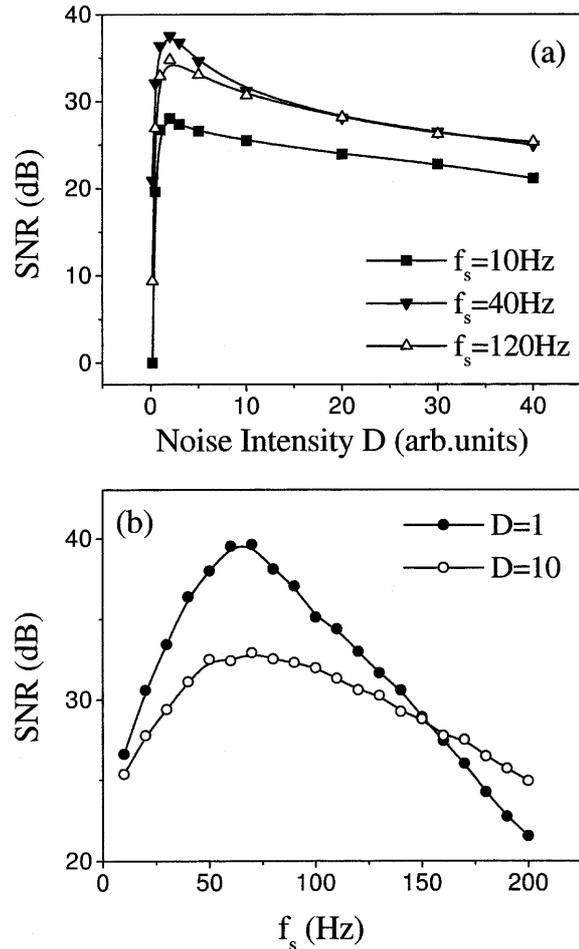 the noise), though it is still modulated by the periodic signal. Thus, the SNR first rises and reaches its maximum at an optimal noise level and then drops as the noise intensity increases. It is worth noting that for large noise intensities there exists a long plateau in the curve. According to the definition of $V^{\text{out}}(t)$, we assume that the average of the firings of all neurons strengthens the periodic feature of the output of the network, and averages out the random feature of firings of the individual neurons. Thus, the SNR of the network has a large value and does not drop as fast as that of the individual neurons at a large noise level. Furthermore, due to the existence of a frequency sensitive range, the SNRs for $f_{\text{s}} = 40\,\text{Hz}$ are always larger than those for $f_{\text{s}} = 10$ and 120 Hz. This is shown clearly in Fig. 7a.

Obviously the frequency sensitivity also depends on the noise intensity; when the noise is large, the sensitivity decreases. Figure 7b shows the SNRs of the network for different signal frequencies in the case of different noise intensities, with $D = 1$ and $D = 10$. It is clear that at a low noise level, the SNRs for frequencies in the range of 30–100 Hz have large values due to the cooperation of the intrinsic oscillation with the periodic signal. This result may make the neuronal system more sensitive to
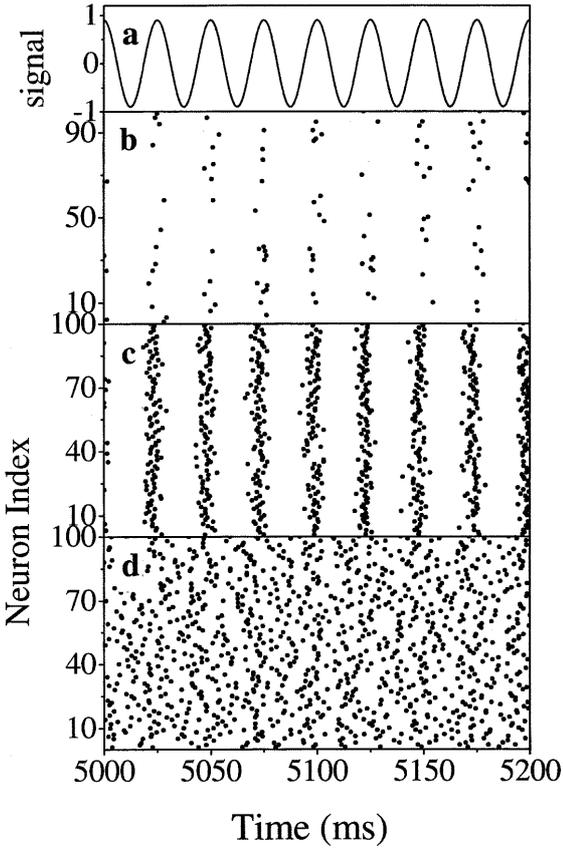
Fig. 8a–d. The periodic signal and the firings of the neurons versus time: **a** The periodic signal with $I_1 = 0.9$ and $f_s = 40$ Hz; **b, c** The Spatiotemporal firing pattern is plotted by recording the firing time t_n^i defined by $V^i(t_n^i) > 0$ mV and $V^i(t_n^{i-}) < 0$ mV. The vertical axes are the neuron index. The noise intensities are $D = 0.5$ for **b**, $D = 2$ for **c**, and $D = 20$ for **d**. The coupling strength is $g_{syn} = 0.5$ mS/cm^2

signals with these frequencies. Furthermore, the signal frequency corresponding to the maximum SNR is about 60 Hz, which coincides with the result mentioned in Sect. 3. However, in the case of large noise, the difference in the SNRs between various frequencies becomes small, because the stochastic nature of the strong noise dominates the firing dynamics. Thus the frequency sensitivity decays at a high noise level (e.g., see the data for the noise intensity $D = 10$ in Fig. 7b).

Now let us check features of the firing neurons in the network. We find that there exists an optimal noise intensity with which the coupled network has a better behavior of synchronization and a large value of the SNR. Figure 8 shows spatiotemporal firing patterns for the case of a signal with $f_s = 40$ Hz and with different noise intensities. Clearly, the neurons fire synchronously with the same period as the signal at a low noise level (see Fig. 8b and c). The combination of the intrinsic oscillation and the input signal makes the neurons ready for firing, once a small noise is added (Wang et al. 1998; Liu et al. 1999). The firing maintains a strong coherence with the signal, that is, the neurons tend to fire a single spike when the signal is around its maximum. Thus the network presents a strong spatiotemporal synchronization. Both $I_{syn}(t)$ and $V^{out}(t)$ present sharp peaks and

vary periodically, resulting in a high SNR. However, in the case of large noise (See Fig. 8d), the effective stimulus strength is rather large, so that the neurons fire more randomly and the firing dynamics presents a stochastic nature. As a result, the spatiotemporal synchronization becomes weak or even is destroyed. The output $V^{out}(t)$ contains an evidently random component that makes the SNR drop quickly. There are many properties of the single neuron and the neuronal network that affect the population synchronization of the network such as the synaptic decay time constant, the synaptic reversal potential, and the ratio of the inhibitory couplings to the excitatory ones. Here we keep all above properties unchanged and only examine the effect of different noise intensities on the synchronous firings of the neuronal network.

The spatiotemporal synchronization is modulated mainly by the resonance between the periodic signal and the intrinsic oscillation, and also by the nonlinear spatiotemporal summation of the post-synaptic potentials. The intrinsic oscillation and the spatiotemporal summation are the intrinsic features of the neurons themselves. The periodic signal makes the neurons fire synchronously, which is strengthened in the presence of couplings. At a suitable noise level, the system shows high SNR, implying that the responses of the neuronal network to an input signal is optimized. Thus, the resonance between the intrinsic oscillation and periodic signal makes the firing of the neurons phase-lock to the input signal, leading to synchronized firing. We would like to point out that the network tends to fire more synchronously when the frequency of the input signal falls into the range of frequency sensitivity (where the system shows high SNR). When stimulated by a signal of low frequency, the neurons need little spatiotemporal summation time in order to fir, due to the long duration of the signal staying around its maximum. The neurons fire nearly every period of the signal, which is beneficial to synchronous firings. However, in the case of a signal with high frequency, the firing of the neurons may be interrupted for several signal periods because the neurons need a longer spatiotemporal summation time. Thus the network presents a weak synchronization. In summary, the network presents a strong spatiotemporal when the SNR is around its maximum.

5 Conclusion

In this paper the intrinsic oscillations and the frequency sensitivity in weak signal detection have been studied via numerical simulations. We started with a general neuronal model, the HH neuronal model, and constructed a globally coupled neuronal network to investigate the physical mechanism underlying frequency sensitivity. The unusual frequency characteristics of the input threshold have been illustrated and explained with inherent oscillations in excitable systems, such as HH neuronal system. The intrinsic oscillations do exist in excitable neurons when the stimuli are both subthreshold and suprathreshold. The CR in a single neuron reflects

the existences of intrinsic oscillations (which could induce the neuron to fire by noise). The existence of the intrinsic oscillatory behavior (e.g., a focus-type state of equilibrium) is a necessary condition for peaks to occur in the PSD at a non-zero frequency, and has a significant effect on the responses of the neuronal system to a subthreshold periodic signal plus white noise. The CR is a nonlinear effect that results from the interaction between the intrinsic oscillatory behavior of the system and noise, and the CR is also affected by the input stimuli.

When subjected to periodic signals, the SNRs of either a single neuron or a network have been studied and are found to present the typical characteristic of the SR. Particularly, a frequency-sensitive range of 30–100 Hz for weak signal detection is found. For signals with frequencies within such a range, the SNRs have large values, implying that the neuronal system is more sensitive to these signals. Furthermore, the couplings between neurons in the network have the effect of an enhancement in the ability to detect and transduce signals.

We would like to emphasize that the range of the frequency sensitivity can not be determined precisely, and its quantitative limits do depend on the details of the neuronal model. However, our results do demonstrate that such a frequency sensitivity results from the resonance between the intrinsic oscillation and the periodic input signal, and that the couplings between neurons have an effect on the improvement for this sensitivity. Furthermore, the network tends to fire more synchronously when the frequency of an input signal falls within the frequency-sensitive range. Indeed, resonance between the intrinsic oscillation and the periodic signal facilitates the synchronization of the network.

In conclusion, the existence of the sensitive frequency range may be of functional significance for signal processing. It may have the effect of an enhancement of the ability to detect and transduce weak signals when frequencies fall within such a range, and also may have an effect on the encoding of these signals. The frequency sensitivity has actually been experimentally demonstrated (Levin and Miller 1996), and our modelling study presented here could be a theoretical interpretation. Finally, it is worth noting that the importance of the intrinsic oscillation underlying frequency sensitivity to other nonlinear systems needs further examination.

References

Bezrukov SM, Vodyarov I (1995) Noise-induced enhancement of signal transduction across voltage-dependent ion channels. Nature 378: 362–364

Bulsara AR, Schmera G (1993) Stochastic resonance in globally coupled nonlinear oscillators. Phys Rev E 47: 3734–3737

Collins JJ, Imhoff TT, Grigg P (1996a) Noise-enhanced tactile sensation. Nature (London) 383: 770

Collins JJ, Imhoff TT, Grigg P (1996b) Noise-enhanced information transmission in rat SA1 cutaneous mechanoreceptors via aperiodic stochastic resonance. J Neurophysiol 76: 642–645

Cordo P, Inglis JT, Verschueren S, Collins JJ, Merfeld DM, Roseblum S, Buckley S, Moss F (1996) Noise in human muscle spindles. Nature 383: 769–770

Douglass JK, Wilkens L, Pantazelou E, Moss F (1993) Noise enhancement of information transfer in crayfish mechanoreceptors by stochastic resonance. Nature (London) 365: 337–340

Fox RF (1991) Second-order algorithm for the numerical integration of colored-noise problems. Phys Rev A 43: 2649–2654

Gammaitoni L, Hänggi P, Jung P, Marchesoni F (1998) Stochastic resonance. Rev Mod Phys 70: 223–287

Gluckman BG, Netoff TI, Neel EJ, Ditto WL, Spano ML, Schiff SJ (1996) Stochastic resonance in a neuronal network from mammalian brain. Phys Rev Lett 77: 4098–4101

Hänggi P, Talkner P, Borkovec M (1990) Reaction-rate theory: fifty years after Kramers. Rev Mod Phys 62: 251–341

Hansel D, Mato G, Meunier C (1993) Phase dynamics for weakly coupled Hodgkin-Huxley neurons. Europhys Lett 23: 367–372

Hodgkin AL, Huxley AF (1952) A quantitative description of membrane current and its application to conduction and excitation in nerve. J Physiol (Lond) 117: 500–544

Hu G, Ditzinger T, Ning CZ, Haken H (1993) Stochastic resonance without external periodic force. Phys Rev Lett 71: 807–810

Lee SG, Alexander N, Seunghwan K (1998) Coherence resonance in a Hodgkin–Huxley neuron. Phys Rev E 57: 3292–3297

Lee SG, Seughwan K (1999) Parameter dependence of stochastic resonance in the stochastic Hodgkin–Huxley neuron. Phys Rev E 60: 826–830

Levin JE, Millerr JP (1996) Broadband neural encoding in the cricket cercal sensory system enhanced by stochastic resonance. Nature 380: 165–168

Linder JF, Meadows BK, Ditto WL, Inchiosa ME, Bulsara AR (1996) Array enhanced stochastic resonance and spatiotemporal synchronization. Phys Rev Lett 75: 3–6

Liu F, Wang JF, Wang W (1999) Frequency sensitivity in weak signal detection. Phys Rev E 59: 3453–3460

Moss F, Bulsara A, Shlesingerr MF (eds) (1993) The Proceedings of the NATO Advanced Research Workshop: Stochastic resonance in physics and biology. J Stat Phys 70: 1–512

Pikovsky AS, Kurths J (1997) Coherence resonance without external periodic force. Phys Rev Lett 78: 775–778

Segev I, Fleshan JW, Burke RE (1989) Compartmental models of complex neurons. In: Koch C, Segev I (eds) Methods in Neuronal Modeling. MIT Press, Cambridge, Mass., p 63

Wang W, Yao XX (1992) Dynamical behaviour of the Bonhoeffer-van der Pol model. Commun Theor Phys 18: 265–274

Wang W, Chen G, Wang ZD (1997a) 40-Hz coherent oscillations in neuronal systems. Phys Rev E 56: 3728–3731

Wang JF, Liu F, Wang JY, Chen G, Wang W (1997b) Frequency characteristics of the input thresholds in stochastic resonant systems. Acto physica Sin (Chinese) 46: 2305–2308

Wang W, Wang YQ, Wang ZD (1998) Firing and signal transduction associated with an intrinsic oscillation in neuronal systems. Phys Rev E 57: 2527–2530

Whittington MA, Traub RD, Jefferys JGR (1995) Synchronized oscillation in interneuron networks driven by metabotropic glutamate receptor activation. Nature 373: 612–615

Wiesenfeld K, Moss F (1995) Stochastic resonance and the benefits of noise from ice ages to crayfish and SQUIDs. Nature (London) 373: 33–36

Wiesenfeld K, Pierson D, Pantazelou E, Dames C, Moss F (1994) Stochastic resonance on a circle. Phys Rev Lett 72: 2125–2129